

## MAJOR PAPER

# Quantitation Error in $^1\text{H}$ MRS Caused by $B_1$ Inhomogeneity and Chemical Shift Displacement

Hidehiro Watanabe\* and Nobuhiro Takaya

**Purpose:** The quantitation accuracy in proton magnetic resonance spectroscopy ( $^1\text{H}$  MRS) improves at higher  $B_0$  field. However, a larger chemical shift displacement (CSD) and stronger  $B_1$  inhomogeneity exist. In this work, we evaluate the quantitation accuracy for the spectra of metabolite mixtures in phantom experiments at 4.7T. We demonstrate a position-dependent error in quantitation and propose a correction method by measuring water signals.

**Materials and Methods:** All experiments were conducted on a whole-body 4.7T MR system with a quadrature volume coil for transmission and reception. We arranged three bottles filled with metabolite solutions of N-acetyl aspartate (NAA) and creatine (Cr) in a vertical row inside a cylindrical phantom filled with water. Peak areas of three singlets of NAA and Cr were measured on three  $^1\text{H}$  spectra at three volume of interests (VOIs) inside three bottles. We also measured a series of water spectra with a shifted carrier frequency and measured a reception sensitivity map.

**Results:** The ratios of NAA and Cr at 3.92 ppm to Cr at 3.01 ppm differed amongst the three VOIs in peak area, which leads to a position-dependent error. The nature of slope depicting the relationship between peak areas and the shifted values of frequency was like that between the reception sensitivities and displacement at every VOI.

**Conclusion:** CSD and inhomogeneity of reception sensitivity cause amplitude modulation along the direction of chemical shift on the spectra, resulting in a quantitation error. This error may be more significant at higher  $B_0$  field where CSD and  $B_1$  inhomogeneity are more severe. This error may also occur in reception using a surface coil having inhomogeneous  $B_1$ . Since this type of error is around a few percent, the data should be analyzed with greater attention while discussing small differences in the studies of  $^1\text{H}$  MRS.

**Keywords:** *proton magnetic resonance spectroscopy, quantitation, chemical shift displacement,  $B_1$  inhomogeneity, reception sensitivity*

## Introduction

Proton magnetic resonance spectroscopy ( $^1\text{H}$  MRS) is a noninvasive tool for the detection and quantitation of endogenous tissue metabolites of the human body. Clinical research in  $^1\text{H}$  MRS has been studied to obtain additional useful information in clinical assessment for pathological conditions. The concentration of tissue metabolites is typically considerably lower than that of water. A relatively large voxel size is required for detecting signals of metabolites and their quantitation is

expected in  $^1\text{H}$  MRS. The peak area of a metabolite resonance in a  $^1\text{H}$  spectrum is proportional to the concentration of the metabolite under the condition carefully considered in relaxation factors of  $T_1$  and  $T_2$  and loading factors, etc. The ratios of peak areas between the different metabolites are frequently used for quantitation of  $^1\text{H}$  MRS. The peak areas can also be used for calculating the absolute concentration.

More accurate quantitation may be expected in  $^1\text{H}$  MRS at higher  $B_0$  field having a feature of high signal to noise ratio. While the difference in frequency between chemical shifts is larger than that for a lower  $B_0$  field, the ratio of the coupling constant  $J_{\text{HH}}$  to the chemical shift difference is smaller. The peak patterns of metabolites with coupled spins are simpler, leading to good peak resolution. However, this larger difference in frequency causes a larger chemical shift displacement in slice selection with gradient pulses.

Another problem that arises at the high  $B_0$  field is the stronger  $B_1$  inhomogeneity, which is caused by shortening of

Center for Environmental Measurement and Analysis, National Institutes for Environmental Studies, 16-2 Onogawa, Tsukuba, Ibaraki 305-8506, Japan

\*Corresponding author, Phone: +81-29-850-2138, Fax: +81-29-850-2880, E-mail: hidewata@nies.go.jp

©2017 Japanese Society for Magnetic Resonance in Medicine

This work is licensed under a Creative Commons Attribution-NonCommercial-NoDerivatives International License.

Received: April 18, 2017 | Accepted: August 10, 2017

the radio-frequency (RF) wavelength due to dielectric effects in tissues. The wavelength approaches the size of a tissue size and  $B_1$  inhomogeneity occurs.<sup>1</sup> One of recent important findings about the  $B_1$  field is that the transmission and reception  $B_1$  fields differ even for a transceiver RF coil, represented as  $\mathbf{B}_1^+$  for transmission and  $\mathbf{B}_1^-$  for reception where bold style denotes a complex vector and \* denotes a complex conjugate.<sup>2</sup> The transmission  $B_1$  field of  $\mathbf{B}_1^+$  affects flip angle (FA) of excited magnetization and signals can be detected via the reception  $B_1$  field of  $\mathbf{B}_1^-$  corresponding to the reception sensitivity.<sup>2-5</sup>

In our preliminary phantom experiments at our 4.7T MR system, we had an experience that the measured concentrations of N-acetyl aspartate (NAA) differed a lot among various positions in  $^1\text{H}$  MRS with the internal water reference. The displacement due to chemical shifts and  $B_1$  inhomogeneity may induce differences of signal intensities along the direction of chemical shift in a localized spectrum. The differences in  $B_1$  at various positions may induce differences in patterns of the spectrum, which can cause position-dependent error in quantitation of metabolites.

In this work, we evaluate the quantitation accuracy in the spectra of metabolite mixtures measured at various positions by the localized  $^1\text{H}$  MRS sequence in phantom experiments. Peak areas of the singlets on the phantom spectra at various positions are calculated for the evaluation of quantitation. We also demonstrate that quantitation error may be caused by the chemical shift displacement and inhomogeneity of reception sensitivity. Inhomogeneity in the transmission  $B_1$  field is also discussed. We attempt to correct those quantitation errors by measuring water signals acquired with the shifted carrier frequency.

## Materials and Methods

All the measurements were conducted on a whole-body MR system (INOVA; Agilent, Palo Alto, CA, USA) equipped with a 4.7T magnet with 925 mm bore, with a gradient system of a 35 mT/m and the maximum gradient strength at a rise

time of 350  $\mu\text{s}$  and with second-order shim coils. A quadrature volume transverse electromagnetic (TEM) coil<sup>6</sup> of 300 mm diameter was used for both transmission and reception. While performing the experiments, we used a cylindrical phantom of 150 mm diameter and 170 mm length filled with water and inside it arranged three 50 ml bottles of 40 mm diameter in a vertical row. These three bottles contained chemical reagents of 25 mM NAA and 25 mM creatine (Cr) (Fluka Chemie GmbH, Buchs, Switzerland). Figure 1a shows a schematic of this cylindrical phantom holding three bottles. We calculated the peak areas of three singlets of methyl  $^1\text{H}$  of NAA at 2.01 ppm, methyl  $^1\text{H}$  of Cr at 3.01 ppm and methylene  $^1\text{H}$  of Cr at 3.92 ppm to evaluate the measurement error of the peak areas.

### *Evaluation of measurement error of peak area in $^1\text{H}$ MRS recorded at different positions*

We measured  $^1\text{H}$  MRS signals of the metabolite mixture to evaluate the measurement error of the peak area corresponding to different positions. The pulse sequence was the combination of seven variable power RF pulses with optimized relation delays (VAPOR) scheme of seven chemical shift selective (CHESS) RF pulses followed by crusher gradients interleaved with two outer volume saturation (OVS) modules and localization of stimulated echo acquisition mode (STEAM) sequence, as shown by Tkáč et al.<sup>7</sup> The water suppression was further improved by applying an additional CHESS pulse during the mixing time (TM) period.<sup>7</sup>

Three asymmetric  $90^\circ$  pulses of 2 ms duration were used in the STEAM module and the bandwidth of each  $90^\circ$  pulse was 3375 Hz. The size of a volume of interest (VOI) was  $20 \times 20 \times 20 \text{ mm}^3$  and slice gradient strength was 1687 Hz/cm. The resultant chemical shift displacement was 1.19 mm per ppm at 4.7T.

The value of TE, TM and TR were set to 4 ms, 35 ms and 15 s respectively in all measurements and the number of transient was 32. The acquisition time of free induction decay (FID) was set at 2.5 s and the complex number of points (np) in the time domain was 20000 comprising of

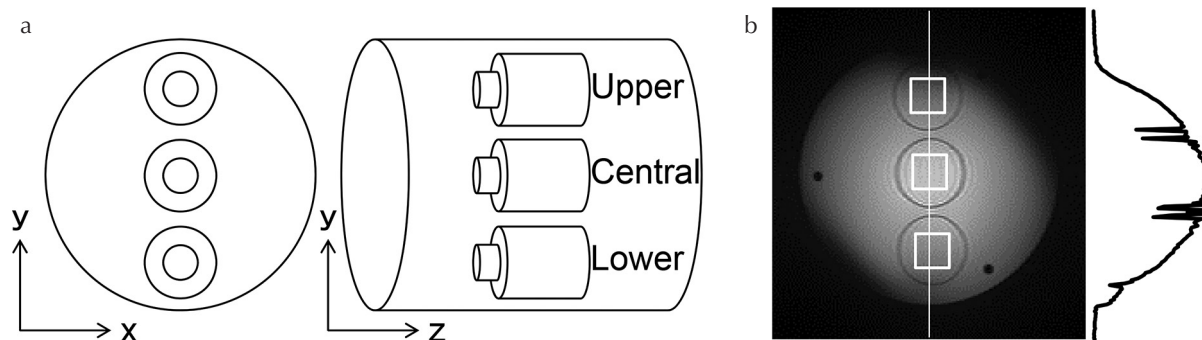


**Fig. 1** A schematic of the phantom used in all the measurements (a). Three 50 ml bottles filled with metabolite mixture of N-acetyl aspartate (NAA) and creatine (Cr) were arranged in a vertical row inside a cylinder of 150 mm diameter and corresponding spectra were measured at the upper, central and the lower volume of interests (VOIs) inside three bottles. An image measured by an adiabatic spin echo sequence to map reception sensitivity<sup>4</sup> where three VOIs were embedded (b).

10000 points each of real and imaginary data. After the FID was zero-filled to 32768 complex data points and applied by the Gaussian window, the one dimensional (1D) spectrum was calculated through Fourier transformation (FT) on the axis of spectral width (SW) with 4 kHz.

Three sets of measurements were performed on the three 50 ml bottles placed at the upper, central and the lower positions. In each measurement, the VOI was defined for the internal volume of each bottle on the scout gradient echo image. The three VOIs corresponding to the upper, central and the lower positions are depicted on the image shown in Fig. 1b and were named as upper, central and lower VOIs. After FASTMAP shimming,<sup>8</sup> the resultant line width of water was obtained as around 3 Hz, measured by the STEAM sequence with the carrier frequency of water <sup>1</sup>H resonance in each measurement. Next, the RF power adjustments were done for 90° slice selective pulses in the STEAM module and for the CHESS pulses in the water suppression module. The metabolite signals were accumulated by the STEAM sequence with the carrier frequency of 3.34 ppm shifted by 1.4-ppm on the lower side of the water resonance of 4.74 ppm. Under this measurement condition, the chemical shifts of the three singlets of methyl <sup>1</sup>Hs of NAA and Cr and methylene <sup>1</sup>H of Cr were -1.33 ppm, -0.32 ppm and 0.58 ppm from the carrier frequency. Slice displacements corresponded to 1.58 mm, 0.38 mm and -0.69 mm. The shifts from the carrier frequency and the corresponding slice displacement were summarized in Table 1.

**Table 1.** Chemical shifts from the carrier frequency and corresponding displacement in singlets of N-acetyl aspartate (NAA) and creatine (Cr)

	CH <sub>2</sub> in Cr 3.92 ppm	N(CH <sub>3</sub> ) in Cr 3.01 ppm	CH <sub>3</sub> in NAA 2.01 ppm
Shift from the carrier frequency [ppm]	0.58	-0.32	-1.33
Slice displacement [mm]	-0.69	0.38	1.58

After eddy current correction and application of the Gaussian window defined as  $\exp(-t/gf)^2$  to accumulated free induction decay (FID) signal, a localized metabolite spectrum was obtained by FT. The value of  $gf$  was adjusted to achieve linewidths of around 7 Hz for the NAA and Cr singlets to compare the spectra of the three VOIs. Then, peak areas of three singlet peaks, the first of NAA at 2.01 ppm, and the two for Cr at 3.01 ppm and at 3.92 ppm were calculated using the integration software including the baseline correction of tilt and dc on VNMR 6.1c (Agilent). These procedures for the measurement and the post processing were performed for the VOIs defined at the upper, central and the lower positions.

### Demonstration of measurement error of peak area caused by chemical shift displacement

For each measurement of the metabolite mixture, we also measured the water signals by the STEAM sequence with shifted carrier frequency to mimic the chemical shift displacement of metabolite peaks as shown in Fig. 2. When a carrier frequency is tuned to water <sup>1</sup>H resonance, no displacement occurs (Fig. 2a). Figure 2b illustrates the sequence condition where the carrier frequency is tuned to a lower side; this mimics the case of methylene <sup>1</sup>H of Cr arising at the higher frequency side. In contrast, Fig. 2c illustrates the condition of methyl <sup>1</sup>H of NAA and Cr on the lower frequency side. The shifts from the carrier frequency were 1.4 ppm, 0.7 ppm, 0 ppm, -0.7 ppm and -1.4 ppm; and the corresponding slice displacements were -1.66 mm, -0.83 mm, 0 mm, 0.83 mm and 1.66 mm respectively (Table 2). After eddy current

**Table 2.** Chemical shifts from the carrier frequency and corresponding displacement in water spectra\*

$\Delta F_{\text{shift}}$ [ppm]	-1.4	-0.7	0	0.7	1.4
Shift from the carrier frequency [ppm]	1.4	0.7	0	-0.7	-1.4
Slice displacement [mm]	-1.66	-0.83	0	0.83	1.66

\*Water spectra were measured by a STEAM sequence with the shifted carrier frequency from the water resonance.  $\Delta F_{\text{shift}}$  is the shifted value, illustrated in Fig. 2.

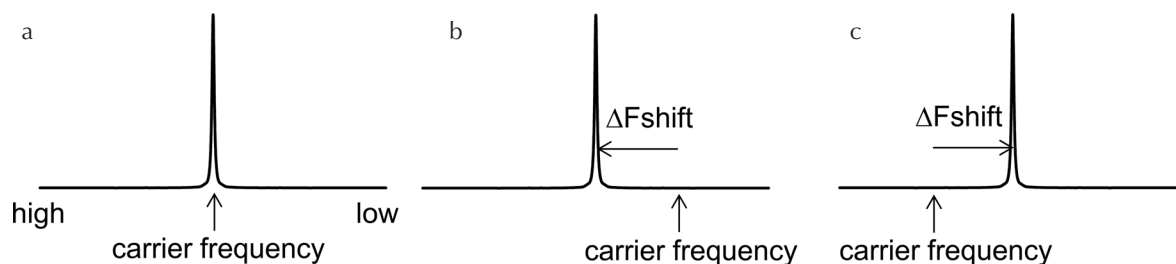


**Fig. 2** Water signal with a stimulated echo acquisition mode (STEAM) sequence with the shifted value of  $\Delta F_{\text{shift}}$  was measured to mimic the chemical shift displacement of metabolite peak. When the carrier frequency is tuned to the water resonance,  $\Delta F_{\text{shift}}$  is equal to zero and non-displacement occurs (a). If that frequency is tuned to the lower side with a negative value of  $\Delta F_{\text{shift}}$ , water resonance arises at the higher frequency side from the carrier frequency, which mimics the peak of methylene proton (<sup>1</sup>H) of creatine (Cr) at 3.92 ppm (b). In contrast, when the frequency is tuned to a higher side with a positive value of  $\Delta F_{\text{shift}}$ , water resonance arises at the lower frequency side, which mimics the peak of N-acetyl aspartate (NAA) at 2.01 ppm (c).

correction and Lorentzian window of 3 Hz were applied to five water signals, the water spectra were calculated by FT. The peak areas of water  $^1\text{H}$  were calculated using the integration software.

### Measurement reception sensitivity profiles from adiabatic spin echo images

For comparing the peak area of the water signals displaced during the slice selection, the reception sensitivity of the cylindrical phantom was measured by an adiabatic spin echo sequence<sup>3,4,9</sup> using the volume transverse electromagnetic (TEM) coil. This imaging sequence consists of an adiabatic half-passage (AHP) pulse for  $90^\circ$  excitation and two adiabatic full-passage (AFP) pulses for refocusing and generating the spin echo signal. Adiabatic pulses offer a means to rotate the magnetization by a constant FA despite the presence of inhomogeneous  $B_1$  field.<sup>10</sup> This feature can generate a homogeneous excitation of magnetization and the image collected from a phantom filled with water represents a map of reception sensitivity.<sup>4</sup>

The measurement condition was set for TE = 26 ms and TR = 4 s. The slice thickness was set at 2.5 mm. A data with matrix size of  $256 \times 96$  was collected for the FOV of  $25.6 \times 19.2 \text{ cm}^2$ . After the time domain data was zero-filled to  $256 \times 256$  and an image was calculated by 2D-FT, the image of  $256 \times 192$  was calculated by the nearest-neighbor interpolation. The resultant image resolution was  $1 \times 1 \text{ mm}^2$ . A transverse image defined by the x and y axes and three coronal images by the z and x axes sliced at the upper, central and lower positions were collected for measuring the reception sensitivity inside the VOI shifted along all the X, Y and Z directions. The axis directions were illustrated in Fig. 1, and all the images were sliced at the center of the VOIs. The pixel intensities were summed up inside each VOI for all the images and subsequently the two sums on transverse and coronal images were multiplied for measuring the

reception sensitivity of each VOI. This procedure was repeated for every 1 mm shifted VOI and a reception sensitivity profile was obtained.

### Correction of error of peak area caused by chemical shift displacement

To decrease the error of peak area, we tried to correct the spectra measured at the upper and the lower VOIs using the measured relationship between the peak area of water and the chemical shift. The correction curve was calculated by curve-fitting the relationship between the reciprocal of the peak area and the chemical shift from the carrier frequency by a third order polynomial expression in each voxel. That correction curve was multiplied to the spectrum in the frequency domain without apodization using Gaussian. This spectrum was obtained by FT directly after the eddy current correction of the accumulated FID signal. Next, corrected FID signal was calculated by the inverse FT. After application of the Gaussian window to the corrected FID, the corrected spectrum was obtained by FT.

## Results

Figure 3 shows the  $^1\text{H}$  spectra of the mixture solution of NAA and Cr. Three singlets of NAA and Cr and complex peak patterns of NAA around 2.6 ppm arose. All spectra of the upper, central and the lower VOIs were normalized by the peak height of methyl  $^1\text{H}$  of Cr at 3.01 ppm. In addition to the standard chemical shift axis, the shift axis from the carrier frequency was also illustrated. The peak height of NAA that appeared at the lower frequency side of the carrier frequency was lower at the upper VOI and higher at the lower VOI, compared with that at the central VOI. This is shown as a dotted line in Fig. 3. In contrast, the peak height of Cr at 3.92 ppm that appeared at the higher frequency side of the carrier frequency was higher at the upper VOI and lower at the lower VOI,

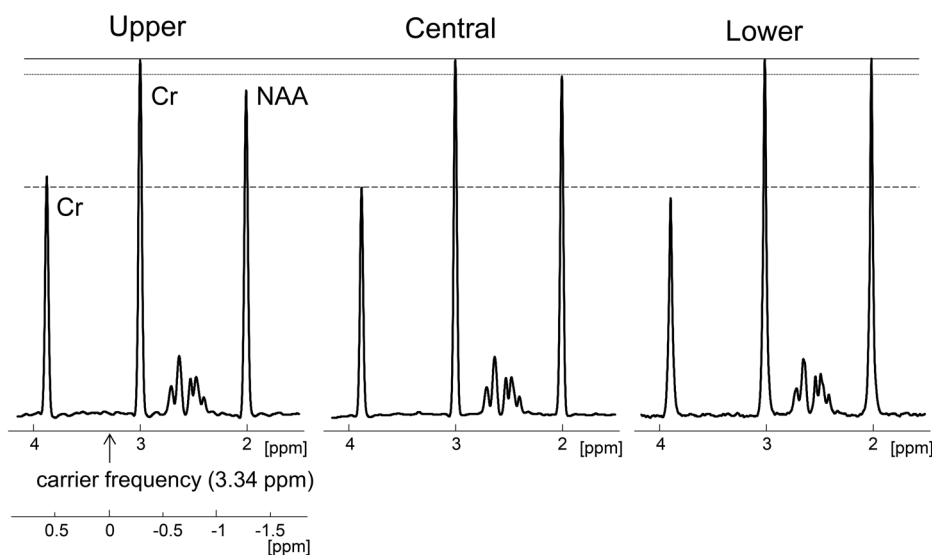


**Fig. 3** Spectra measured at the upper, central and the lower volume of interests (VOIs) from left to right. Gaussian window was applied before fourier transform (FT) to achieve linewidths of around 7 Hz for N-acetylaspartate (NAA) and creatine (Cr) singlets to compare spectra. The peak heights decrease from the upper VOI to the lower VOI in the peak of Cr at 3.91 ppm arising in the higher frequency side from the carrier frequency. In contrast, the peak heights increase from the upper VOI to the lower VOI in the peak of NAA at 2.01 ppm arising in the lower frequency side. The chemical shift axis from the carrier frequency was also shown under the spectra measured at the upper VOI.



compared with that of the central VOI. This is shown as a dashed line in Fig. 3.

Peak areas of those three peaks at three VOIs were summarized in Table 3. All peak areas were normalized by that of Cr at 3.01 ppm. At the upper VOI, the peak area of Cr at 3.92 ppm is 0.67 and that of NAA at 2.01 ppm is 0.93. For the central VOI, the peak area of Cr at 3.92 ppm is 0.65 and that of NAA is 0.96. In contrast with the upper and central VOIs, the peak area at the lower VOI of Cr at 3.92 ppm is 0.63 and that of NAA is 0.99. As a result, a measurement error of the peak area of around  $\pm 3\%$  occurred in all these three VOIs.

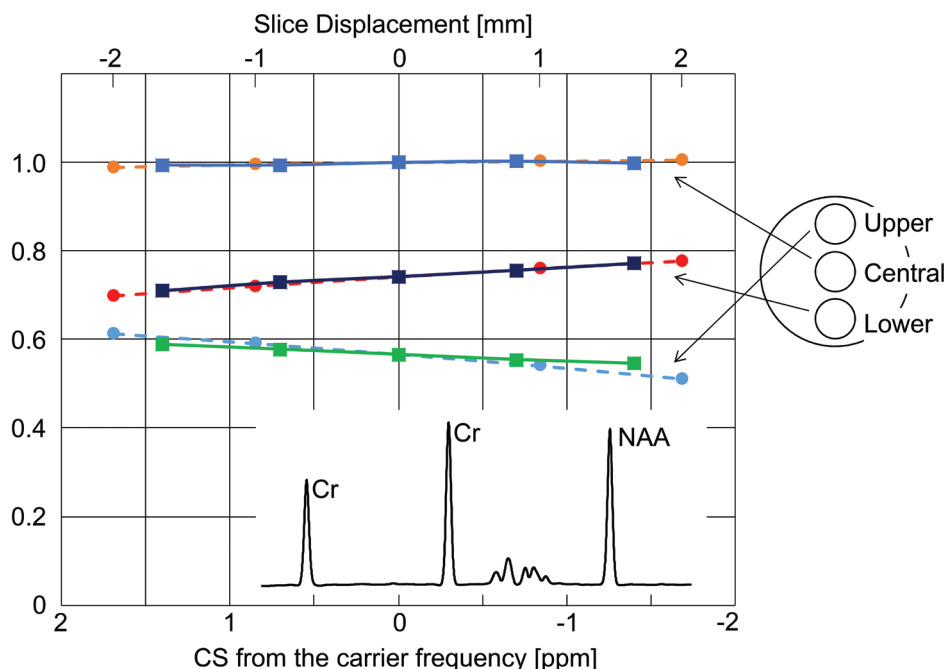
**Table 3.** Peak areas of NAA and Cr in spectra measured at three VOIs

	CH <sub>2</sub> in Cr 3.92 ppm	N(CH <sub>3</sub> ) in Cr 3.01 ppm	CH <sub>3</sub> in NAA 2.01 ppm
Upper	0.67	1.0	0.93
Central	0.65	1.0	0.96
Lower	0.63	1.0	0.99

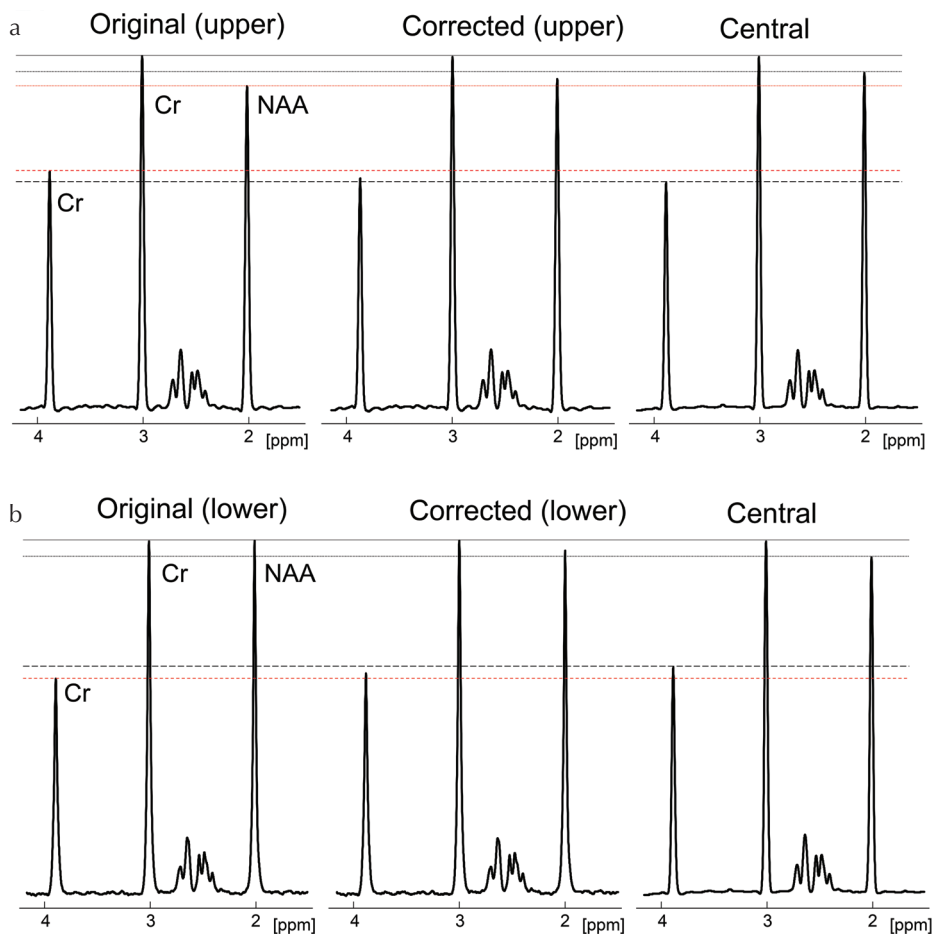
Peak areas were normalized by that of creatine (Cr) at each volume of interest (VOI). Normalized standard deviation was 0.0014 under 5 measurements. NAA, N-acetyl aspartate.

Figure 4 shows the relationships between shifted values from the carrier frequency and the peak areas of water resonances at the upper, central and the lower VOIs. The peak areas of water resonances were normalized by the peak area at the central VOI with a non-shifted carrier frequency of  $\Delta F_{\text{shift}} = 0$  ppm. The typical measured spectrum of NAA and Cr was embedded in this figure. At the upper VOI, the peak area corresponding to the lower frequency side of the carrier frequency is lower than that of the higher frequency side. In contrast, for the lower VOI the peak area for the lower frequency side is higher than that of the higher frequency side. These trends are in coincidence with the spectra of NAA and Cr in Fig. 3 and the peak areas in Table 3.

In addition to those relationships between the shifted values and the peak area, Fig. 4 also shows the relationship between the slice displacement and the reception sensitivity, obtained from the transverse and coronal images measured by the adiabatic spin echo imaging sequence at the three VOIs. The transverse image is shown in Fig. 1b. The reception sensitivity at the non-displaced VOI was resized to match the normalized value of peak area of water resonance with non-shifted carrier frequency at each VOI. Both the profiles of peak area along the shifted value and of the reception sensitivity along the slice displacement show similar patterns at all the three VOIs.



**Fig. 4** The relationships between the shifted values from the carrier frequency and the peak areas of water resonances (closed circle) along with those between the slice displacement and the reception sensitivity (closed square) at the upper, central and the lower volume of interests (VOIs). Normalized standard deviation of water peak area was 0.0026 and that of reception sensitivity was 0.0025 under five measurements. The sensitivity was calculated from transverse and coronal images obtained by the adiabatic spin echo imaging sequence. Peak areas of water resonances were normalized by the peak area at the central VOI with a non-shifted carrier frequency of  $\Delta F_{\text{shift}} = 0$  ppm. The reception sensitivity at non-displacement was resized to that normalized value of peak area of water resonance with  $\Delta F_{\text{shift}} = 0$  ppm at each VOI. The typical measured spectrum of N-acetyl aspartate (NAA) and creatine (Cr) was embedded. At the upper VOI, the peak area at the lower frequency side from the carrier frequency is lower than that at the higher frequency side. In contrast, that at the lower side is higher than that at the higher side. These trends are in coincidence with the spectra of NAA and Cr in Fig. 3 and the peak areas in Table 3. Both the profiles of peak areas along the shifted value and of reception sensitivity along the slice displacement show similar patterns at all the three VOIs.



**Fig. 5** Corrected spectra in the amplitude along the chemical shift axis measured at the upper and the lower volume of interests (VOIs) by the curve calculated from the relationship shown in Fig. 4. The curve was obtained by curve fitting the relationship between the reciprocal of the peak area of water resonance and the chemical shift from the carrier frequency by a third order polynomial expression at each VOI. In the corrected spectrum at the upper (a), and the lower VOI (b), both peak heights of N-acetylaspartate (NAA) at 2.01 ppm and creatine (Cr) at 3.92 ppm grew close to those at the central VOI. Peak areas in the corrected spectra are also shown in Table 4. Differences of peak heights and peak areas of NAA at 2.01 ppm and Cr at 3.92 ppm were decreased; and quantitation accuracy was improved.

**Table 4.** Peak areas of NAA and Cr in corrected spectra at three VOIs

	$\text{CH}_2$ in Cr 3.92 ppm	$\text{N}(\text{CH}_3)$ in Cr 3.01 ppm	$\text{CH}_3$ in NAA 2.01 ppm
Upper	0.65	1.0	0.95
Central	0.65	1.0	0.97
Lower	0.65	1.0	0.96

Peak areas were normalized by that of creatine (Cr) at each volume of interest (VOI). NAA, N-acetyl aspartate.

Figure 5 shows corrected spectra at the upper and the lower VOI. In the both corrected spectrum at the upper (Fig. 5a) and the lower VOI (Fig. 5b), both peak heights of NAA at 2.01 ppm and Cr at 3.92 ppm became close to those of the central VOI. Peak areas in the corrected spectra are also shown in Table 4. Differences of peak heights and peak areas of NAA at 2.01 ppm and Cr at 3.92 ppm were decreased between VOIs; and the quantitation accuracy was improved.

## Discussion

In this work, we measured the dielectric sample of the cylindrical phantom filled with water by the volume TEM coil.

Figure 1b depicts homogeneous  $B_1$  fields around the central region. The pattern of  $B_1$  inhomogeneity where the signal intensity is high in the central region and that is low around the surrounding regions was like that in the human brain.<sup>3</sup> As we can see in Fig. 4, the profile of the reception sensitivity was almost flat; the peak area for the water resonance shifted by the chemical shift displacement was maintained around constant value. In contrast,  $B_1$  fields around the upper and the lower regions were inhomogeneous (Fig. 1b). The profile of the reception sensitivity had a slope of around +2% per mm at the lower VOI and at the upper VOI slope was around -2% (Fig. 4). The relationships between the chemical shifts and the peak areas shift show similar tendencies at both the upper and the lower VOIs (Fig. 4). Figure 3 and Table 3 also show similar tendencies in peak heights and peak areas of methyl  $^1\text{H}$ s of NAA and Cr and methylene  $^1\text{H}$  of Cr. From these findings, we confirmed that the position-dependent error in peak area occurs in a localized  $^1\text{H}$  MRS due to the chemical shift displacement and inhomogeneity of reception sensitivity. As static  $B_0$  field is higher,  $B_1$  inhomogeneity of the human body due to dielectric effects is stronger. Then, this error may be more significant in  $^1\text{H}$  MRS at 7T.

In the quantitation of  $^1\text{H}$  MRS, normalization using the peak area of Cr at 3.01 ppm is frequently used. The

measurement error of peak area due to the chemical shift may give a misleading interpretation of metabolite changes. In the curve fitting with the linear combination model (LCModel<sup>11</sup>) that is also frequently used in quantitation, all peaks of a metabolite are curve fitted for quantitation of that metabolite. As the chemical shifts of those peaks differ, the error in the peak area may cause quantitation error in LCModel fitting.

The amplitude of the slice gradient in the STEAM module was 1687 Hz/cm and the displacement value due to the chemical shift was around 1.19 mm per ppm at 4.7T. Despite the small displacement of around a few mm, the difference of the reception sensitivity reached around a few percent (Fig. 4). This is because that the inhomogeneity of  $B_1$  field directly affects the reception sensitivity.

To evaluate the effect by the inhomogeneity of transmission  $B_1$ ,  $B_1^+$  mapping was done by the phase method.<sup>3,4,12</sup> The amplitude of STEAM signal was calculated by the cube of sine of FA and the signal is proportional to  $B_1^- \sin^3(\alpha B_1^+)$  where  $\alpha$  is coefficient. Then, the estimated error of the peak area of NAA with 1.58 mm slice displacement (Table 1) was 0.6%. The reason of this small effect is that the magnetization is proportional to sine of FA even if a difference of a few percent exists. In addition, the transmission power of the STEAM sequence was adjusted at every VOI in the measurements.

Surface coils are utilized in the reception mode for improving the sensitivity and for parallel imaging in clinical MRI. The error in peak area due to the chemical shift may also occur due to the inhomogeneity of  $B_1$  fields of the surface coil in <sup>1</sup>H MRS. In this situation, we had better a series of water spectra with shifted carrier frequencies to evaluate the error in peak area due to the chemical shift displacement. This measurement will also help in improving the quantitation accuracy as mentioned above.

The measurement of water spectra by the localized sequence with shifted carrier frequency was useful for improvement of quantitation of spectrum. This correction method requires uniform concentration of metabolite inside the VOI displaced by the chemical shift difference. It should be noted that it is an approximation method for the application of *in vivo* studies. The value of chemical shift displacement is at most around few mm. When we pay attention to the size and the position of the VOI, the difference of concentration metabolite between the VOI and the shifted VOI may be small even for *in vivo* studies, such as in the measurements performed in human brain. In this situation, this approximation method may also be useful to improve the quantitation.

## Conclusion

The chemical shift displacement and the inhomogeneity of reception sensitivity cause amplitude modulation along the chemical shift direction on a localized spectrum in <sup>1</sup>H MRS.

This leads to a quantitation error of the metabolite. A few percent error may occur in quantitation. Then, when small difference is observed in clinical studies using <sup>1</sup>H MRS, we should consider data with attention and should measure a series of water spectra with shifted carrier frequency in order to evaluate this error. The series of water spectra may be useful in correcting the amplitude modulation and accuracy of quantitation may be subsequently improved. This error is more significant at higher  $B_0$  field where chemical shift displacement and  $B_1$  inhomogeneity are more severe. The error may also occur in reception using a surface coil having inhomogeneous  $B_1$  field.

## Conflicts of Interest

We declare that we have no conflict of interest.

## References

- Vaughan JT, Garwood M, Collins CM, et al. 7T vs. 4T: RF power, homogeneity, and signal-to-noise comparison in head images. *Magn Reson Med* 2001; 46:24–30.
- Hoult DI. The principle of reciprocity in signal strength calculations—a mathematical guide. *Concepts Magn Reson* 2000; 12:173–187.
- Watanabe H. Investigation of the asymmetric distributions of RF transmission and reception fields at high static field. *Magn Reson Med Sci* 2012; 11:129–135.
- Watanabe H. Experimental demonstration of the proportionality of the RF reception field to a complex conjugate of  $B_1^-$ . *Magn Reson Med Sci* 2012; 11:193–196.
- Collins CM, Yang QX, Wang JH, et al. Different excitation and reception distributions with a single-loop transmit-receive surface coil near a head-sized spherical phantom at 300 MHz. *Magn Reson Med* 2002; 47:1026–1028.
- Vaughan JT, Hetherington HP, Otu JO, Pan JW, Pohost GM. High frequency volume coils for clinical NMR imaging and spectroscopy. *Magn Reson Med* 1994; 32:206–218.
- Tkáč I, Starcuk Z, Choi IY, Gruetter R. *In vivo* <sup>1</sup>H NMR spectroscopy of rat brain at 1 ms echo time. *Magn Reson Med* 1999; 41:649–656.
- Gruetter R, Tkáč I. Field mapping without reference scan using asymmetric echo-planar techniques. *Magn Reson Med* 2000; 43:319–323.
- Mitsumori F, Watanabe H, Takaya N, Garwood M. Apparent transverse relaxation rate in human brain varies linearly with tissue iron concentration at 4.7 T. *Magn Reson Med* 2007; 58:1054–1060.
- Tannús A, Garwood M. Adiabatic pulses. *NMR Biomed* 1997; 10:423–434.
- Provencher SW. Estimation of metabolite concentrations from localized *in vivo* proton NMR spectra. *Magn Reson Med* 1993; 30:672–679.
- Lee Y, Han Y, Park H, Watanabe H, Garwood M, Park JY. New phase-based  $B_1$  mapping method using two-dimensional spin-echo imaging with hyperbolic secant pulses. *Magn Reson Med* 2015; 73:170–181.